

# **Modelling of Automotive Engine Dynamics using Diagonal Recurrent Neural Network**

**Yujia Zhai**

(AI University Research Centre (AI-URC), Xi'an Jiaotong-Liverpool University  
Suzhou, China  
yujia.zhai@xjtlu.edu.cn)

**Kejun Qian**

(Suzhou Power Supply Company, Suzhou, China  
kejun.qian@xjtlu.edu.cn)

**Fei Xue**

(Xi'an Jiaotong-Liverpool University, Suzhou, China  
fei.xue@xjtlu.edu.cn)

**Moncef Tayahi**

(Xi'an Jiaotong-Liverpool University, Suzhou, China  
moncef.tayahi@xjtlu.edu.cn)

**Abstract:** The spark-ignition (SI) engine dynamics is described as a severely nonlinear and fast process. A black-box model obtained by system identification approach is often valuable for the control and fault diagnosis application on such systems. Recurrent neural network (RNN) might be better suited for such dynamical system modelling due to its feedback back scheme if compared with feed-forward neural network. However, the computational load for RNN limits its practical application. In this paper, a diagonal recurrent neural network (DRNN) is investigated to model SI engine dynamics to achieve a balance between the modelling performance and computational burden. The data collection procedure and algorithms for training DRNN are presented too. Satisfactory results on modelling have been obtained with moderate cost on computation.

**Keywords:** Diagonal Recurrent Neural Network, Dynamical System Modelling; Spark-Ignition Engine, System Identification

**Categories:** H.3.1, H.3.2, H.3.3, H.3.7, H.5.1

## **1 Introduction**

Internal combustion engines have been widely used in automotive industry for many years. However, due to the increasing requirement from governments to protect the global environment, the modelling and control on such system have become the most complex problems for control system engineers and university researchers, who have been striving to reduce substantially emissions and fuel consumption while maintaining the best engine performance [Balluchi, 00][ [Nicolao, 96]]. To satisfy these requirements, a variety of variables need to be controlled, such as engine speed, engine torque, spark ignition timing, fuel injection timing, air intake, air-fuel ratio

(AFR) and so on [Tan, 00] [Vinsonneau, 03]. These variables are complicatedly related to each other. Control methods that are based on dynamics models have been successfully implemented in many practical industrial applications.

With the development of high speed micro-controller, more and more advanced modelling techniques can be introduced into the area of automotive engine control [Behrouz, 12]. Neural networks are powerful in their ability on representing both linear and nonlinear relationships and learning the relationships directly from the input-output data of dynamical systems. Recurrent neural networks (RNN) have important capabilities, which are not found in feed-forward networks, such as attractor dynamics and the ability to store information for later use. Of particular interest is their ability to deal with time varying input or output through their own natural temporal operation [Zhai, 10]. Thus, the RNN is a dynamic mapping and is better suited for dynamic systems modelling than the feed-forward networks. Many advanced researches have been done on neural modelling of engine systems in last two decades [Gertler, 95] [Krishnaswami, 95] [Nyberg, 97] [Hsu, 95] [Nyberg, 98] [Kim, 98]. More recently, ARSIE showed a procedure to enhance identification of recurrent neural networks for simulating air/fuel ratio dynamics in SI engines [Arsie, 06]. However, due to the limitation of computational power, the practical applications of engine controllers using recurrent neural network are still very limited [Vigraham, 06]. Therefore, considering the computation burden for fast dynamic system, the DRNN can be a suitable choice for the design of automotive engine management system, instead of fully connected recurrent neural networks (FRNN). DRNN has one hidden layer, and the hidden layer is comprised of self-recurrent neurons. Since there is no inter-links among neurons in the hidden layer, DRNN has considerably fewer weights than FRNN and the network is simplified considerably [Zhai, 09].

In this paper, a DRNN structure and dynamic back-propagation training algorithm are introduced in for in Section 2. A mean value engine model used in this research is shown in Section 3. The modelling procedure and modelling results are provided in Section 4. Based on the results obtained, a conclusion is given in Section 5.

## 2 DRNN Structure and Algorithms

### 2.1 DRNN Structure

The DRNN consists of one hidden layer of computation nodes. The basic DRNN structure is shown in Figure. 1,

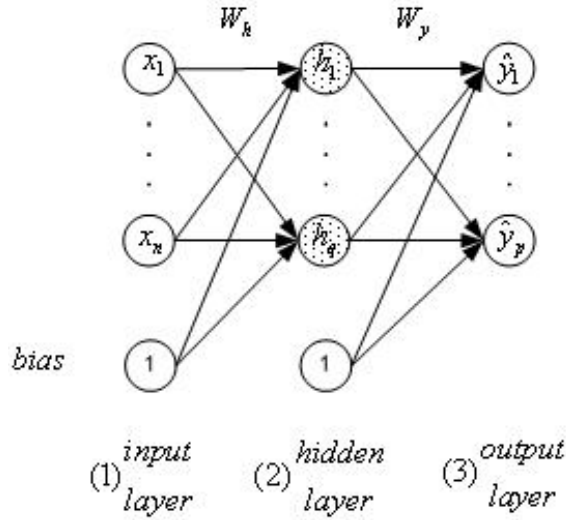


Figure 1: DRNN structure.

where  $x(k) \in \mathbb{R}^n$ ,  $h(k) \in \mathbb{R}^q$ ,  $\hat{y}(k) \in \mathbb{R}^p$ ,  $W^h(k) \in \mathbb{R}^{q \times (n+1)}$ ,  $W^d(k) \in \mathbb{R}^{v \times q}$  and  $W^y(k) \in \mathbb{R}^{p \times (q+1)}$

$$W^h = \begin{bmatrix} w_1^h \\ \vdots \\ w_q^h \end{bmatrix} = \begin{bmatrix} w_{1,1}^h & \cdots & w_{1,n+1}^h \\ \vdots & \ddots & \vdots \\ w_{q,1}^h & \cdots & w_{q,n+1}^h \end{bmatrix} \tag{1}$$

$$W^y = \begin{bmatrix} w_1^y \\ \vdots \\ w_p^y \end{bmatrix} = \begin{bmatrix} w_{1,1}^y & \cdots & w_{1,q+1}^y \\ \vdots & \ddots & \vdots \\ w_{p,1}^y & \cdots & w_{p,q+1}^y \end{bmatrix} \tag{2}$$

$$W^d = \begin{bmatrix} (w_1^d)^T \\ \vdots \\ (w_v^d)^T \end{bmatrix} = \begin{bmatrix} w_{1,1}^d & \cdots & w_{1,q}^d \\ \vdots & \ddots & \vdots \\ w_{v,1}^d & \cdots & w_{v,q}^d \end{bmatrix} \tag{3}$$

- $x_i$  the  $i$ th node in the input layer,  $i=0, 1, \dots, n$ .
- $h_i$  output of the  $i$ th node in the hidden layer,  $i=0, 1, \dots, q$ .
- $\hat{y}_i$  output of the  $i$ th node in the output layer,  $i=0, 1, \dots, p$ .
- $w_{ij}^h$  weight linking the  $j$ th node in the input layer to the  $i$ th node in the hidden layer,

$w^d_{ij}$   $i=1, 2, \dots, q$ , and  $j=0, 1, \dots, n+1$ .  
 recurrent weight linking the  $i$ th order time delay of the  $j$ th node in the hidden layer,  
 $i=1, 2, \dots, v$ , and  $j=0, 1, \dots, q$ .  
 $w^y_{ij}$  weight linking the  $j$ th node in the hidden layer to the  $i$ th node in the output layer,  
 $i=1, 2, \dots, p$ , and  $j=0, 1, \dots, q+1$ .

The recurrent structure in the hidden layer node is feedback to the hidden neuron itself with time delay after activation function.

In mathematical terms, the DRNN with  $q$  hidden layer nodes is governed by the following equations.

$$\hat{y}(k) = W^y \begin{bmatrix} h(k) \\ 1 \end{bmatrix} \tag{4}$$

$$h(k) = f[z(k)] \tag{5}$$

$$z(k) = W^h \begin{bmatrix} x(k) \\ 1 \end{bmatrix} + \begin{bmatrix} w^d_{1,1} & \dots & 0 \\ \vdots & \ddots & \vdots \\ 0 & \dots & w^d_{1,q} \end{bmatrix} \dots \begin{bmatrix} w^d_{v,1} & \dots & 0 \\ \vdots & \ddots & \vdots \\ 0 & \dots & w^d_{v,q} \end{bmatrix} \begin{bmatrix} h^d(k-1) \\ \vdots \\ h^d(k-v) \end{bmatrix} \tag{6a}$$

$$= W^h \begin{bmatrix} x(k) \\ 1 \end{bmatrix} + \begin{bmatrix} \text{diag}(w^d_1) & \dots & \text{diag}(w^d_v) \end{bmatrix} \begin{bmatrix} h^d(k-1) \\ \vdots \\ h^d(k-v) \end{bmatrix} \tag{6b}$$

$$h^d(k) = h(k), \quad \text{feedback} \tag{7}$$

where  $f(\cdot)$  is the non-linear activation function in hidden layer. The typical hidden layer activation functions used in DRNN are sigmoid and hyperbolic tangent function. In the investigation of process modelling with DRNN, only sigmoid activation function is chosen as the non-linear transfer function in DRNN.

**2.2 DRNN Training using Dynamic Back-Propagation Algorithm**

Let  $y(k)$  and  $\hat{y}(k)$  be the actual responses of the plant and the output of the DRNN model, then an error function for a training cycle for DRNN can be defined as

$$E_m = \frac{1}{2} (y(k) - \hat{y}(k))^2 \tag{8}$$

The gradient of error simply becomes

$$\frac{\partial E_m}{\partial W} = -e_m(k) \frac{\partial \hat{y}(k)}{\partial W} \quad (9)$$

where  $e_m(k) = y(k) - \hat{y}(k)$  is the output error between the plant and the DRNN.

Given the DRNN shown in Figure 1 and described by the equations (1)-(7), the output gradients with respect to output, recurrent and input weights, respectively, are given by

$$\frac{\partial \hat{y}(k)}{\partial W^y} = h(k) \quad (10)$$

$$\frac{\partial \hat{y}(k)}{\partial W^d} = W^y P(k) \quad (11)$$

$$\frac{\partial \hat{y}(k)}{\partial W^h} = W_j^y Q(k) \quad (12)$$

Where  $P(k) = \frac{\partial h(k)}{\partial W^d}$  and  $Q = \frac{\partial h(k)}{\partial W^h}$  and satisfy

$$P(k) = f'(z) (h(k-1) + W^d P(k-1)) \quad (13)$$

$$Q(k) = f'(z) (x(k) + W^D Q(k-1)) \quad (14)$$

The weights can now be adjusted following a gradient method, i.e., the update rule of the weights becomes

$$W(k+1) = W(k) + \eta \left( -\frac{\partial E_m}{\partial W} \right) \quad (15)$$

where  $\eta = [\eta^h \ \eta^d \ \eta^y]$  is the learning rate. The equations (8)-(15) define the dynamic back-propagation algorithm (DBP) for DRNN.

The update rule call for a proper choice of the learning rate  $\eta$ . If we let  $\eta^h$ ,  $\eta^d$ , and  $\eta^y$  be the learning rate for DRNN weights  $W^h$ ,  $W^d$ , and  $W^y$  respectively, then, the DBP algorithm converges if  $0 < |W_j^d| < 1$ ,  $j = 1, 2, \dots, \nu$  and the learning rate are chosen as:

$$0 < \eta^y < \frac{2}{q} \quad (16)$$

$$0 < \eta^d < \frac{2}{q} \left[ \frac{1}{W_{\max}^y} \right]^2 \quad (17)$$

$$0 < \eta^h < \frac{2}{(n+q)} \left[ \frac{1}{W_{\max}^y \cdot x_{\max}} \right]^2 \quad (18)$$

Here  $q$  is the number of recurrent neurons in the hidden layer,  $n$  is the number of inputs to the DRNN,  $W_{\max}^y := \max_k \|W^y(k)\|$ ,  $x_{\max} := \max_k \|x(k)\|$  and  $\|\cdot\|$  is the sup-norm.

### 3 SI Engine Dynamics

In both industrial practice and scientific research, it has been more popular to use engine simulation models to make engine system analysis and design because it is much more economical than using a real engine test bed. The engine model adopted in this paper is referred to as the mean value engine model (MVEM) developed by Hendricks [Zhai, 09], which is a widely used benchmark for engine modeling and control. The three distinct subsystems of this model are the fuel injection, manifold filling and the crankshaft speed dynamics and those systems are modeled independently. Since this MVEM can achieve a steady state accuracy of about  $\pm 2\%$  over the entire operating range of the engine, it is extremely useful for validation of control strategies using simulation. A full description of the MVEM can be found in [Zhai, 09].

#### 3.1 Manifold Filling Dynamics

The intake manifold filling dynamics are analyzed from the viewpoint of the air mass conservation inside the intake manifold. It includes two nonlinear differential equations, one for the manifold pressure and the other for the manifold temperature. The manifold pressure is mainly a function of the air mass flow past throttle plate, the air mass flow into the intake port, the exhaust gas re-circulation (EGR) mass flow, the EGR temperature and the manifold temperature. It is described as

$$\dot{p}_i = \frac{\kappa R}{V_i} (-\dot{m}_{ap} T_i + \dot{m}_{at} T_a + \dot{m}_{EGR} T_{EGR}) \quad (19)$$

The manifold temperature dynamics are described by the following differential equation

$$\dot{T}_i = \frac{RT_i}{p_i V_i} \left[ -\dot{m}_{ap} (\kappa - 1) T_i + \dot{m}_{at} (\kappa T_a - T_i) \right] + \dot{m}_{EGR} (\kappa T_{EGR} - T_i) \quad (20)$$

In equation (1) and (2), the air mass flow dynamics in the intake manifold can be described as follows. The air mass flow past throttle plate  $\dot{m}_{at}$  is related with the throttle position and the manifold pressure. The air mass flow into the intake port  $\dot{m}_{ap}$  is represented by a well-known speed-density equation:

$$\dot{m}_{at}(u, p_i) = m_{at1} \frac{p_a}{\sqrt{T_a}} \beta_1(u) \beta_2(p_r) + m_{at0} \quad (21)$$

$$\dot{m}_{ap}(n, p_i) = \frac{V_d}{120RT_i} (\eta_i \cdot p_i) n \quad (22)$$

where

$$\beta_1(u) = 1 - \cos(u) - \frac{u_0^2}{2!} \quad (23)$$

$$\beta_2(p_r) = \begin{cases} \sqrt{1 - \left(\frac{p_r - p_c}{1 - p_c}\right)^2}, & \text{if } p_r \geq p_c \\ 1, & \text{if } p_r < p_c \end{cases} \quad (24)$$

$$p_r = \frac{p_i}{p_a} \quad (25)$$

and  $m_{at0}$ ,  $m_{at1}$ ,  $u_0$ ,  $p_c$ , are constants. Additionally, instead of directly model the volumetric efficiency  $\eta_i$ , it is easier to generate the quantity  $\eta_i \cdot p_i$  which is called normalized air charge. The normalized air charge can be obtained by the steady state engine test and is approximated with the polynomial equation (8)

$$\eta_i \cdot p_i = s_i(n) p_i + y_i(n) \quad (26)$$

where  $s_i(n)$  and  $y_i(n)$  are positive, weak functions of the crankshaft speed and  $y_i \ll s_i$

### 3.2 Crankshaft Speed Dynamics

The crankshaft speed is derived based on the conservation of the rotational energy on the crankshaft

$$\dot{n} = -\frac{1}{In} \left( P_f(p_i, n) + P_p(p_i, n) + P_b(n) \right) + \frac{1}{In} H_u \eta_i(p_i, n, \lambda) \dot{m}_f(t - \Delta\tau_d) \quad (27)$$

Both the friction power  $P_f$  and the pumping power  $P_p$  are related with the manifold pressure  $p_i$  and the crankshaft speed  $n$ . The load power  $P_b$  is a function of the crankshaft speed  $n$  only. The indicated efficiency  $\eta_i$  is a function of the manifold pressure  $p_i$ , the crankshaft speed  $n$  and the air fuel ratio  $\lambda$ .

### 3.3 Fuel Injection Dynamics

According to Hendrick's identification experiments with SI engine, the fuel flow dynamics could be described as following equations [Gertler, 95]

$$\dot{m}_{ff} = \frac{1}{\tau_f} (-\dot{m}_{ff} + X_f \dot{m}_{fi}) \quad (28)$$

$$\dot{m}_{fv} = (1 - X_f) \dot{m}_{fi} \quad (29)$$

$$\dot{m}_f = \dot{m}_{fv} + \dot{m}_{ff} \quad (30)$$

where the model is based on keeping track of the fuel mass flow. The parameters in the model are the time constant for fuel evaporation,  $\tau_f$ , and the proportion  $X_f$  of the fuel which is deposited on the intake manifold,  $\dot{m}_{ff}$ , or close to the intake valves,  $\dot{m}_{fv}$ . These parameters are operating point dependent and thus the model is nonlinear in spite of its linear form, which could be approximately expressed in terms of the states of the model as

$$\tau_f(p_i, n) = 1.35 \times (-0.672n + 1.68) \times (p_i - 0.825)^2 + (-0.06 \times n + 0.15) + 0.56 \quad (31)$$

$$X_f(p_i, n) = -0.277p_i - 0.055n + 0.68 \quad (32)$$

## 4 SI Engine Modelling by DRNN

### 4.1 Data Collection

In order to analyze the modeling performance of DRNN in practical driving conditions, two sets of random amplitude signals (RAS) were designed for throttle angle bounded between 20 and 70 degree, and the fuel injection between 0.0014 kg/sec and 0.0079 kg/sec, which are shown in Figure 2 and Figure 3. These two sets of data were introduced into the mean value engine model described in Section 3. Then, from the model output, the intake manifold pressure, temperature, engine speed, air fuel ratio can be obtained with the same size of data as input data.

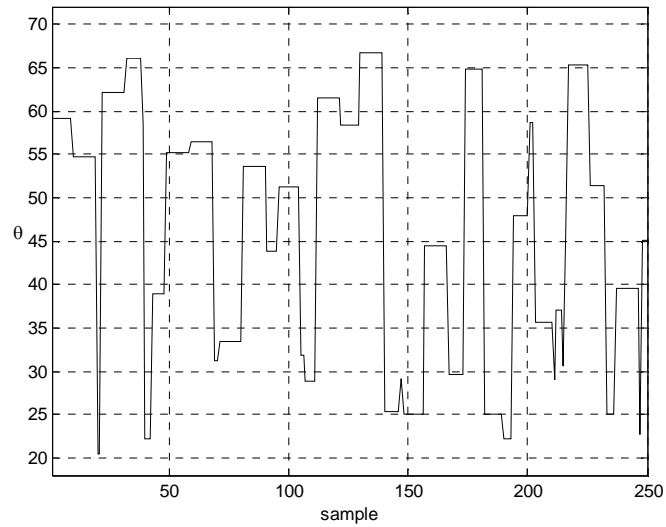


Figure 2: RAS for Throttle Angle

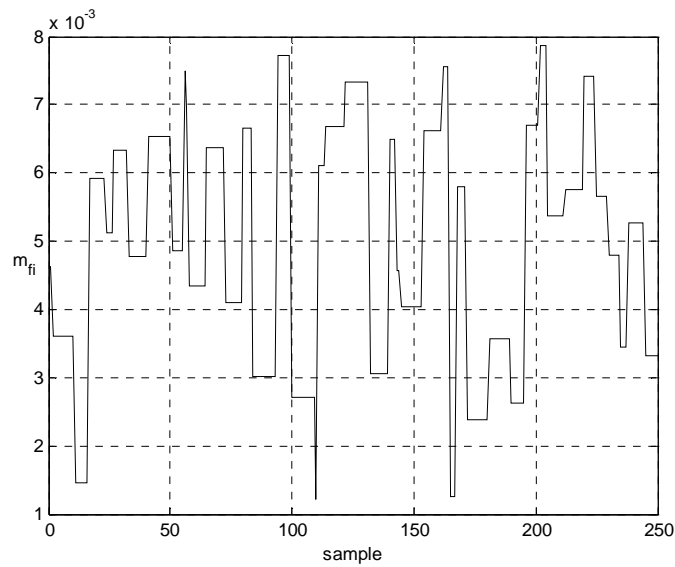


Figure 3: RAS for  $m_{fi}$

The sample time in the simulation was set to 0.1s. The simulated engine model MVEM was run for 500s with a set of 5000 data samples collected for all input and output variables. These data were divided into two groups. The first 4000 samples

were used for DRNN training and the other 1000 samples for testing the modelling performance.

### 4.2 Engine Modelling

In this section, a multi-input and multi-output engine model by DRNN is constructed. From the engine simulation mentioned in last section, four variables were chosen to be the network inputs: fuel injection  $\dot{m}_{fi}$ , throttle angle  $u$ , air-fuel ratio  $y$ , and engine speed  $n$ . Since there is no systematical way to identify the optimal order of input data and the best network size, different orders of the plant input/output and numbers of hidden nodes have been tried in the experiments and a second-order structure with 15 hidden nodes given minimum prediction error is selected. Therefore, the DRNN structure can be shown in Figure 4, which constructs a second-order engine model with 8 inputs and two outputs.

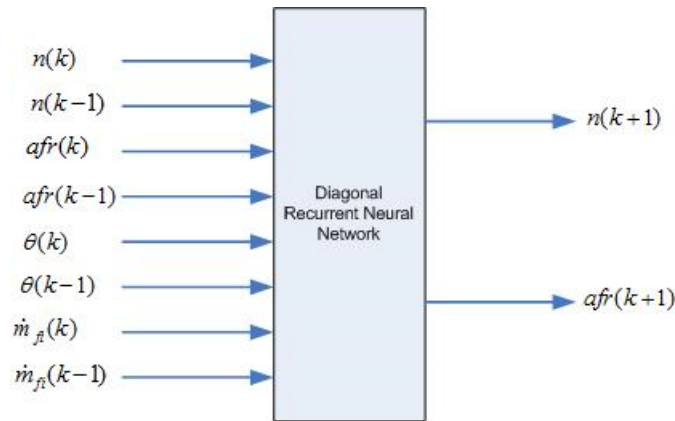


Figure 4: The structure of the DRNN engine models

The DBP algorithms mentioned were used for training the DRNN. The modeling results are shown in Figure 5 and Figure 6.

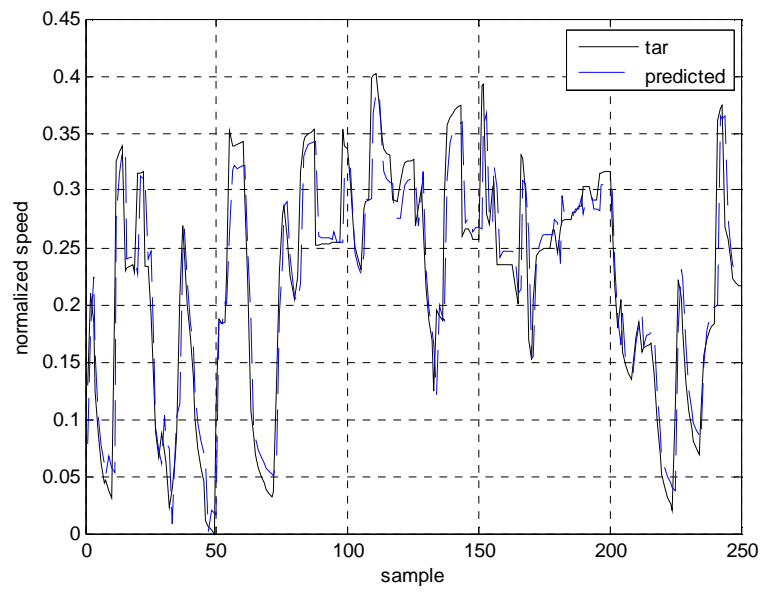


Figure 5: Engine speed modeling result

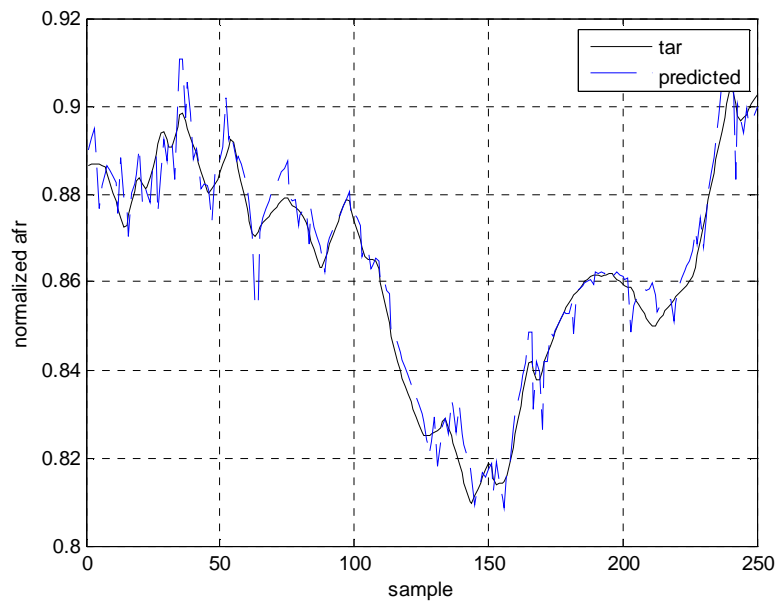


Figure 6: Air fuel ratio modeling result

The mean absolute error (MAE) as shown in equation 33, is adopted to evaluate the modeling performance.

$$\text{MAE} = \frac{1}{n} \sum_{i=1}^n |f_i - y_i| = \frac{1}{n} \sum_{i=1}^n |e_i| \quad (33)$$

The MAE for engine speed modeling is 0.0224, and the MAE for air fuel ratio modeling is 0.0035. It can be seen that, with the small size of DRNN, the SI engine dynamics could be accurately represented by the MIMO DRNN model.

## 5 Conclusions

1) A DRNN as a type of recurrent network can catch the fast and nonlinear dynamics of automotive engine accurately. A proper engine model structure based on DRNN has been obtained and tested on MVEM.

2) The modelling result obtained in this paper has shown that DRNN can be a suitable model for the control and fault diagnosis in product ECU in next generation.

### Acknowledgements

This research was financially supported by the Centre for Smart Grid and Information Convergence (CeSGIC) and the XJTLU Key Programme Special Fund (KSF-P-02) at Xi'an Jiaotong-Liverpool University. The authors would like to thank all the parties concerned.

### References

- [Arsie, 06] Ivan Arsie, Cesare Pianese, and Marco Sorrentino, A procedure to enhance identification of recurrent neural networks for simulating air–fuel ratio dynamics in SI engines , *Engineering Applications of Artificial Intelligence*, Volume 19, Issue 1, February 2006, Pages 65-77
- [Balluchi, 00] Balluchi A, Benvenuti L, Di Benedetto MD, Pinello C, Sangiovanni-Vincentelli AL. Automotive engine control and hybrid systems: Challenges and opportunities. *Proceeding of the IEEE*, 2000, 88(7), 888-912.
- [Behrouz, 12] Behrouz Ebrahimi, Reza Tafreshi, Houshang Masudi, Matthew Franchek, Javad Mohammadpour, Karolos Grigoriadis, A parameter-varying filtered PID strategy for air–fuel ratio control of spark ignition engines, *Control Engineering Practice*, Volume 20, Page 805-815, 2012
- [Gertler, 95] J. Gertler, M. Costin, X. Fang, R. Hira, Z. Kowalczyk, M. Kunwer, and R. Monajemy, Model based diagnosis for automotive engines—Algorithm development and testing on a production vehicle, *IEEE Trans. Contr. Syst. Technol.*, vol. 3, pp. 61–69, Jan. 1995.
- [Hsu, 95] P. L. Hsu, K. L. Lin, and L. C. Shen, Diagnosis of multiple sensor and actuator failures in automotive engines, *IEEE Trans. Veh. Technol.*, vol. 44, pp. 779–789, July 1995.
- [Kim, 98] Y.W. Kim, G. Rizzoni, and V. Utkin, Automotive engine diagnosis and control via nonlinear estimation, *IEEE Contr. Syst. Mag.*, pp. 84–99, Oct. 1998.

- [Krishnaswami, 95] V. Krishnaswami, G. C. Luh, and G. Rizzoni, Nonlinear parity equation based residual generation for diagnosis of automotive engine faults, *Contr. Eng. Practice*, vol. 3, no. 10, pp. 1385–1392, 1995.
- [Nicolao, 96] De Nicolao G., Scattolini R. and Siviero C. Modelling the volumetric efficiency of IC engines: parametric, non-parametric and neural techniques. *Control Eng. Practice*, 1996, 4(10), 1405-1415.
- [Nyberg, 97] M. Nyberg and L. Nielsen, Model based diagnosis for the air intake system of the SI engine, in *SAE Paper*, (970 209), 1997.
- [Nyberg, 98] M. Nyberg and A. Perkovic, Model based diagnosis of leaks in the air-intake system of an SI-engine, in *SAE Paper* 980 514, 1998.
- [Tan, 00] Tan Yonghong and Mehrdad Saif, Neural-networks-based nonlinear dynamic modeling for automotive engines. *Neurocomputing*, 2000, 30, 129-142.
- [Vigraham, 06] Vigraham, S.A., Gallagher, J.C., CTRNN-EH in Silicon: Challenges in Realizing Configurable CTRNNs in VLSI, *Evolutionary Computation*, 2006. CEC 2006. IEEE Congress on Vancouver, BC, 2006 , pp. 2807-2813
- [Vinsonneau, 03] Vinsonneau J. A. F., Shields D. N., King P.J. and Burnham K. J. Polynomial and neural network spark ignition engine intake manifold modeling. *Proc. 16th Int. Conf. on Systems Engineering, ICSE'*, 2003, 2,718-723.
- [Zhai, 09] Yu-Jia Zhai, Ding-Li Yu, Neural network model-based automotive engine air/fuel ratio control and robustness evaluation, *Engineering Applications of Artificial Intelligence*, Volume 22, Issue 2, Pages 171-180, 2009
- [Zhai, 10] Yu-Jia Zhai, Ding-Wen Yu, Hong-Yu Guo, Ding-Li Yu, Robust air/fuel ratio control with adaptive DRNN model and AD tuning, *Engineering Applications of Artificial Intelligence*, Volume 23, Issue 2, Pages 283-289, 2010.